Design of robust optimal PI controller for PMSM servo drives

R. MARY LOURDE, L. UMANAND AND N. J. RAO
CEDT, IISc., Bangalore, email : mary@cedt.iisc.ernet.in

Indexing terms: PMSM servo drive, optimal controller, Robust controllers.

Abstract

Vector controlled PMSM servo drive is a MIMO full state feedback system. Since only the measurable quantities are used as the feedback to the controller, the whole problem is treated as a linear quadratic tracker (LQT) with output feedback for the purpose of designing the optimum controller to meet the given specifications. The performance of the optimal controller is evaluated by studying the transient and steady state response to step changes in reference speed. The sensitivity of each current and speed loop controllers to changes in motor parameters and load torque are investigated. A torque observer is used for the feedforward torque control to make the optimal controller robust against load torque variations.

Major discipline: Electrical Machines and adjustable speed drives(5).

1. Introduction

The control of electrical motors used in high performance servo drives and robots demand control concepts that can achieve high dynamics and the prescribed accuracy for all operating conditions. The class of reference input signals, external disturbances, parameter variations and the power source characteristics define the operating conditions of the servo drive. Among AC motors, the permanent magnet synchronous motor (PMSM) has a high power density and torque to inertia ratio, because of the use of high quality rare-earth magnetic materials, that make it the most popular choice for replacing DC motors for servo applications in the power range of 1–10 kW[9]. The PMSM with sinusoidal flux distribution is preferred over the one with trapezoidal flux distribution due to lower torque ripple. Generally the control design is based on linear models with the assumption that the mechanical and electrical time constants differ atleast by one order of magnitude which result in series control structures. In many industrial drives, the vector controlled PMSM with current controlled voltage source inverter and PI speed regulator has been used as high performance servo systems. The PI controller is simple and easy to implement. Also it is known that it can yield attractive controller performance and robustness properties. Such controllers reject constant external disturbances, and has good low frequency disturbance response properties. The overall performance of the drive system depends ultimately on the selection of the controller parameters. However, as application fields of servo systems expand, various high-grade demands for speed control characteristics arise. For example the spindle of an NC machine is required to maintain constant speed under fluctuating

load torque conditions, a robotic arm should be able to maintain its velocity and trajectory in-spite of variations of moment of inertia etc.

The conventional PI controller design is based on the linear SISO systems control tech-niques. However vector controlled PMSM is a MIMO system which has a non-linear model and it exhibits coupled dynamics. This paper presents the design of controller for a PMSM by opti-mal control methods. The performances of the controllers for a wide operating range are evalu-ated. The sensitivity of the controllers to plant parameter variations and load torque variations are compared.

2. Vector control of PMSM and the motor dynamics

Control of PMSM can be achieved either through closed loop field oriented control, where the two physical quantities generating the torque i.e. the flux and the current are kept orthogo-nal to each other or through the open loop control without field orientation such as v/f control. In the field oriented control of PMSM the flux producing component of the stator current is made zero and the torque component of the stator current is made orthogonal to the magnetic flux. Field orientation gives good dynamic performance but suffers from poor disturbance rejection at low speeds. In servo control problem this implies that the error in speed caused by a torque disturbance is independent of the speed at which the motor is running. On the other hand in v/f control the field disorientation gives better disturbance rejection (i.e. small peak deviation from set speed) at low speeds. But the transient response is inferior to the field ori-ented control. The block diagram for the field oriented speed control of a PMSM is shown in the Figure 2.1

The torque is controlled by the I_{sq} loop and the flux by the I_{sd} loop. The speed is controlled by the outer loop. The torque and speed dynamics of the vector controlled PMSM is shown in equations (2.1)[3].

FIG. 2.1. Field oriented control schematic of a speed controlled PMSM drive.

$$V_{sd}(t) = R_s I_{sd}(t) + L_s \frac{d}{dt} I_{sd}(t) - \omega_s L_s I_{sq}(t)$$

$$V_{sq}(t) = R_s I_{sq}(t) + L_s \frac{d}{dt} I_{sq}(t) + \omega_s L_s I_{sd}(t) + K_E \omega_r(t)$$

$$T_e = K_T I_{sq} \text{ and } T_e - T_L = J_m \frac{d}{dt} \omega_r + B_m \omega_r \qquad (2.1)$$

From the equations (2.1) it can be seen that the d- and q- axis equations have cross coupling terms. These cross coupling effects becomes significant at higher speeds and can be cancelled by feedforward compensations as shown in the Figure 2.1, to achieve decoupled control of d- and q- axis currents.

The error between the commanded and actual speed is operated upon by the speed PI controller that will decide the required current reference for the torque. In the constant air gap flux mode of operation, the direct axis reference current I_{sdref} is made zero. PI controllers are used as current controllers. The error generated by comparing the demanded current with the actual current of the motor, is passed on to the current controller. The output of the current controller with proper decoupling gives the necessary reference voltages in the d-q axis reference frame. These voltages are then transformed into stationary reference frame and are given as the reference voltages to the inverter. A 1 kHz sine-triangle PWM inverter is used. The maximum lag of the inverter can be half the period of the carrier frequency. i.e., 0.5 msec and the motor electrical time constant is 8.2 msec. In practice, antialiasing filters are used to filter the measurement noise that occurs at frequencies greater than 50KHz. The bandwidth of the system is 122 rad/sec. The frequency of antialiasing filter is fixed as 490 rad/sec without loss of information. The motor parameters used for the simulation is shown in the appendix I. Applications such as machine tool drive require fast response to step change in speed without any overshoot. So the speed controller design is aimed at critical damping and the settling time less than 100 msec.

3. Optimal control

Due to the interaction of the control loops in a multivariable system, even though each SISO transfer function can have acceptable properties with step response and robustness, the coordinated motion control of the system can fail to be acceptable[4]. By using modern control techniques, many of the limitations of the classical controls for multivariable feedback control systems can be overcome. Modern control designs use fundamentally time domain technique whereas classical control designs use frequency domain technique. In the modern controller synthesis using state feedback technique, all the states must be available for feedback. To overcome this difficulty, output feedback is used. Further unlike the full state feedback, the output feedback control law allows any desired dynamical control structure, thereby regaining much of the intuition of classical control design[2,12].

For a MIMO system, eigenvalues and eigenvectors are to be assigned to the closed loop feedback system to achieve some desired dynamical transient response characteristics[5]. In a multivariable system, eigenvectors determine the shape of the response modes and the eigen-

values determine the domain characteristics of the response. In servo drive control it is always desirable to have a time invariant response, in which the convergence characteristics of the system are clearly known to the users. The closed loop eigenstructure assignment technique has been used in the design of state feedback control law for effective shaping of the time response for MIMO time invariant systems[5]. In such systems the designs always lead to unique feedback gain matrix because of the time invariance. But this method is inadequate when it is used to formulate a feedback control law for a MIMO time varying PMSM system described in equation (2.1) where the system matrix keeps changing with the speed of the system (ω_r). To maintain the time invariant response mode, a varying eigenstructure assignment has to be carried out.

An alternate approach to the eigen structure assignment technique is the optimal control[2]. When applied to a MIMO time varying system, the optimal control designs transfer the iterations on eigenvalues and eigenvectors to the iterations on elements in a cost function J. The resultant optimised designs will achieve some compromise between the use of the control effort and the response, and at the same time guarantees a stable system. Each iteration on the parameters in J produces a candidate design that can be evaluated considering the specifications. To achieve the optimal controller, a linear quadratic performance criterion of states and inputs are minimised. For standard discrete LQT with output feedback problems, the performance index used is

$$ J = \frac{1}{2} \sum_{k=0}^{\infty} \left(\hat{x}_k^T . Q . \hat{x}_k + \hat{u}_k^T . R . \hat{u}_k \right) + \frac{1}{2} \bar{e}^T . V . \bar{e} + \frac{1}{2} \sum_i \sum_j \left(g_{ij} . k_{ij}^2 \right) \tag{3.1} $$

where $\hat{x}$ and $\hat{u}$ are state and input deviations respectively, Q is the state weighing matrix, R is the input weighing matrix, $\bar{e}$ is the steady state error, V the steady state error weighing matrix and g_{ij} the weight of the gain element k_{ij} of the gain matrix K. In the present case, because of the PI structure of the controller, the steady state error will be zero and hence the corresponding term in the performance index can be made zero. For the selected controller structure it can be seen that this is a special case of output feedback that is also a full state feedback. However the linear quadratic tracker with output feedback approach is used to obtain the optimum gains.

The stability margins of the linear quadratic regulator in the continuous-time cases are infinity and 60degrees for gain and phase respectively[12]. Although discrete time optimal linear quadratic regulators have margins inferior to continuous-time case, guaranteed phase and gain margins have been obtained[10]. The deficiency of the stability margins arises only in cases where the optimal feedback gains are very large. So it cannot occur in discrete-time case and the stability margins will thus provide a reliable indication of the robustness of the corresponding discrete-time optimal regulator.

4. Formulation of PMSM drive as an optimal control problem

The dynamic model of PM machine transformed to the d-q reference frame[5] in continuous state space form is given by equation (4.1).

$$\frac{d}{dt}\begin{bmatrix} I_{sd} \\ I_{sq} \end{bmatrix} = \begin{bmatrix} -R_s/L_s & \omega_s \\ -\omega_s & -R_s/L_s \end{bmatrix}\begin{bmatrix} I_{sd} \\ I_{sq} \end{bmatrix} + \begin{bmatrix} 1/L_s & 0 \\ 0 & 1/L_s \end{bmatrix}\begin{bmatrix} V_{sd} \\ V_{sq} \end{bmatrix} \tag{4.1}$$

Which is in the form $x_p = A_p.x_p + B_p.u_p$; $y_p = C_p.x_p + D_p.u_p$ where

$$A_p = \begin{bmatrix} -R_s/L_s & \omega_s \\ -\omega_s & -R_s/L_s \end{bmatrix} \text{ and } B_p = \begin{bmatrix} 1/L_s & 0 \\ 0 & 1/L_s \end{bmatrix}; C_p = \begin{bmatrix} 1 & 0 \\ 0 & 1 \end{bmatrix}; D_p = \begin{bmatrix} 0 & 0 \\ 0 & 0 \end{bmatrix}$$

The plant states and outputs are $x_p = y_p = [I_{sd}\ I_{sq}]^T$;

Inputs to the plant are $u_p = [V_{sd}\ V_{sq}]^T$;

Since an anti-aliasing filter is also used in the control path to filter out the high frequency noises such as measurement noise, the dynamics of the anti-aliasing filter should be included in the system formulation. Here a low pass filter of the form $H_a(s) = a/(s + a)$ is used. For the motor details indicated in the Appendix-I, the bandwidth is 122 rad/sec. The filter frequency is selected as 490 rad/sec. The anti-aliasing filter dynamics represented by the matrices A_a, B_a, C_a and D_a are

$$A_a = \begin{bmatrix} -a & 0 \\ 0 & -a \end{bmatrix}; B_a \begin{bmatrix} a & 0 \\ 0 & a \end{bmatrix}; C_a = \begin{bmatrix} 1 & 0 \\ 0 & 1 \end{bmatrix}; D_a = \begin{bmatrix} 0 & 0 \\ 0 & 0 \end{bmatrix};$$

The filter states and outputs are $x_a = y_a = [I_{sda}\ I_{sqa}]^T$;

The input to the filter are $u_a = [I_{sd}\ I_{sq}]^T$;

The filter states augmented plant G_{pa} is described by the matrices A_{pa}, B_{pa}, C_{pa} and D_{pa} which is given by

$$A_{pa} = \begin{bmatrix} a_{pa11} & a_{pa12} \\ a_{pa21} & a_{pa22} \end{bmatrix} \quad [4 \times 4\,\text{matrix}]; a_{pa11} = A_p...[2\times 2]; \quad \text{where } a_{pa12} = 0\ [2 \times 2];$$

$$a_{pa22} = A_a... [2 \times 2]; \qquad\qquad a_{pa21} = \begin{bmatrix} a & 0 \\ 0 & a \end{bmatrix}..... [2 \times 2];$$

$$B_{pa} = \begin{bmatrix} b_{pa11} \\ b_{pa21} \end{bmatrix}...[4 \times 2];$$

where $b_{pa11} = B_p... [2 \times 2];$ $\qquad\qquad b_{pa21} = 0.... [2 \times 2];$

The states of G_{pa} are $x_{pa} = [x_p\ x_a]^T$; input to G_{pa} are $u_{pa} = u_p$; and outputs are $y_{pa} = y_a$

The augmented plant $G_{pa}(s)$ is transformed into the discrete domain using the ZOH equivalent transformation to obtain $G_{pa}(z)$. The transformed G_{pa} must be augmented to the discrete current controller dynamics.

The digital current controller structure for the PMSM drive is as shown in the Fig. 4.1. The dynamics of PMSM that is transformed into the discrete domain and the dynamics of the compensators form a part of system formulation. The sampling frequency of the current loop is
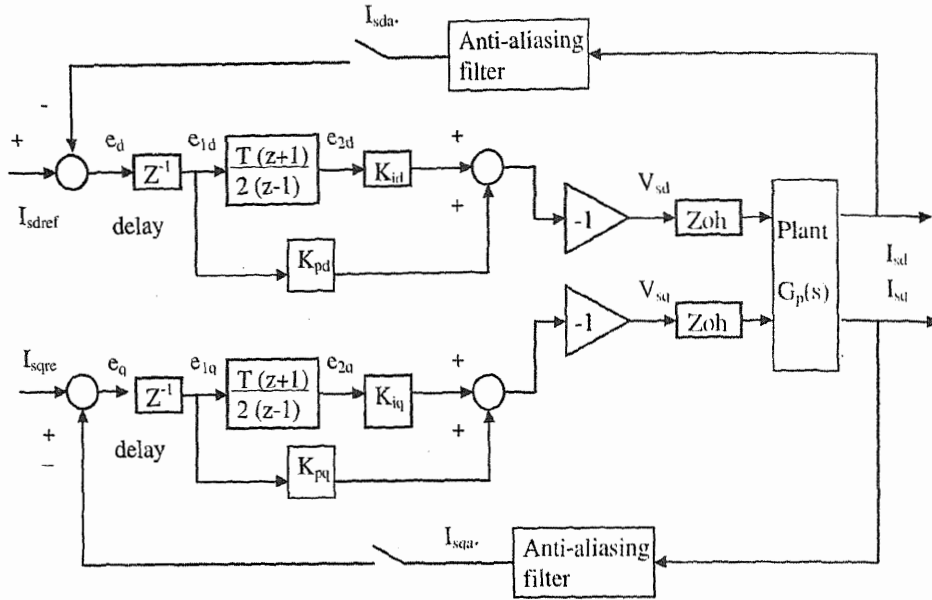
R. MARY LOURDE, *et al.*

FIG. 4. 1 Digital current controller structure for PMSM

selected as 5 kHz. The delays due to computations and the inverter lag are taken care of by introducing a sample delay at each of the current loops.

Referring to the Fig. 4.1, the delay dynamics can be represented as

$$\begin{bmatrix} e_{1d} \\ e_{1q} \end{bmatrix}_{k+1} = \begin{bmatrix} -I_{sda} \\ -I_{sqa} \end{bmatrix}_k + \begin{bmatrix} I_{sdref} \\ I_{sqref} \end{bmatrix}_k \tag{4.2}$$

and the PI dynamics can be represented as

$$\begin{bmatrix} e_{2d} \\ e_{2q} \end{bmatrix}_{k+1} = \begin{bmatrix} \dfrac{T}{2} e_{1d} & e_{2d} \\ \dfrac{T}{2} e_{1q} & e_{2q} \end{bmatrix}_k + \begin{bmatrix} \dfrac{T}{2} e_{1d} \\ \dfrac{T}{2} e_{1q} \end{bmatrix}_{k+1} \tag{4.3}$$

where T is the sampling time of the analog current feedback signal.

Combining the equations (4.2) and (4.3), the compensator dynamics G_c can be written as

$$\begin{bmatrix} e_{1d} \\ e_{1q} \\ e_{2d} \\ e_{2q} \end{bmatrix}_{k+1} = \begin{bmatrix} 0 & 0 & 0 & 0 \\ 0 & 0 & 0 & 0 \\ \dfrac{T}{2} & 0 & 1 & 0 \\ 0 & \dfrac{T}{2} & 0 & 1 \end{bmatrix} * \begin{bmatrix} e_{1d} \\ e_{1q} \\ e_{2d} \\ e_{2q} \end{bmatrix}_k + \begin{bmatrix} -1 & 0 & 1 & 0 \\ 0 & -1 & 0 & 1 \\ -\dfrac{T}{2} & 0 & \dfrac{T}{2} & 0 \\ 0 & -\dfrac{T}{2} & 0 & \dfrac{T}{2} \end{bmatrix} * \begin{bmatrix} I_{sda} \\ I_{sqa} \\ I_{sdref} \\ I_{sqref} \end{bmatrix}_k \tag{4.4}$$

i.e. $x_c(k + 1) = A_c\, x_c(k) + B_c u_c(k)$; where

$$A_c = \begin{bmatrix} 0 & 0 & 0 & 0 \\ 0 & 0 & 0 & 0 \\ \dfrac{T}{2} & 0 & 1 & 0 \\ 0 & \dfrac{T}{2} & 0 & 1 \end{bmatrix} \text{ and } B_c = \begin{bmatrix} -1 & 0 & 1 & 0 \\ 0 & -1 & 0 & 1 \\ -\dfrac{T}{2} & 0 & \dfrac{T}{2} & 0 \\ 0 & -\dfrac{T}{2} & 0 & \dfrac{T}{2} \end{bmatrix}$$

The states of G_c are $x_c = [e_{1d}\ e_{1q}\ e_{2d}\ e_{2q}]^T$;

the inputs to G_c are $u_c = [I_{sda}\, I_{sqa}\, I_{sdref}\, I_{sqref}]^T$; and the outputs of the G_c are $y_c = x_c$.

Augmenting the compensator G_c to the plant-filter G_{pa} dynamics, the total system dynamics G is obtained. If the complete system is represented in the form

$$x_{k+1} = A.\ x_k + B.\ u_k + E.\ r_k;\ y_k = C.\ x_k + F.\ r_k\ ;\ z_k = H.\ x_k \qquad (4.5)$$

$$A = \begin{bmatrix} a_{11} & a_{12} \\ a_{21} & a_{22} \end{bmatrix}...[8 \times 8]; where\ a_{11} = A_{pa}...[4 \times 4];$$

$$a_{21} = \begin{bmatrix} 0 & 0 & -1 & 0 \\ 0 & 0 & 0 & -1 \\ 0 & 0 & -\dfrac{T}{2} & 0 \\ 0 & 0 & 0 & -\dfrac{T}{2} \end{bmatrix}; a_{12} = 0...[4 \times 4]; a_{22} = A_c...[4 \times 4];$$

$$B = \begin{bmatrix} b_{11} \\ b_{21} \end{bmatrix}...[8 \times 2]; where\ b_{11} = B_{pa}...[4 \times 2]; b_{21} = 0...[4 \times 2];$$

$$E = \begin{bmatrix} e_{11} \\ e_{21} \end{bmatrix}...[8 \times 2]; where\ e_{11} = 0...[4 \times 2]; e_{21} = \begin{bmatrix} 1 & 0 \\ 0 & 1 \\ \dfrac{T}{2} & 0 \\ 0 & \dfrac{T}{2} \end{bmatrix}$$

$$C = \begin{bmatrix} 0 & 0 & 0 & 0 & 1 & 0 & 0 & 0 \\ 0 & 0 & 0 & 0 & 0 & 1 & 0 & 0 \\ 0 & 0 & 0 & 0 & 0 & 0 & 1 & 0 \\ 0 & 0 & 0 & 0 & 0 & 0 & 0 & 1 \end{bmatrix}; F = 0...[4 \times 2];$$

The augmented total system is shown in the Fig. 4.2. The system states, inputs, reference inputs and outputs respectively are

$x = [x_{pa}\ x_c]^T...[8 \times 1];\ u = u_{pa} = u_p....[2 \times 1];\ r = [I_{sdref}\, I_{sqref}]^T;\ y = y_c..[4 \times 1];$
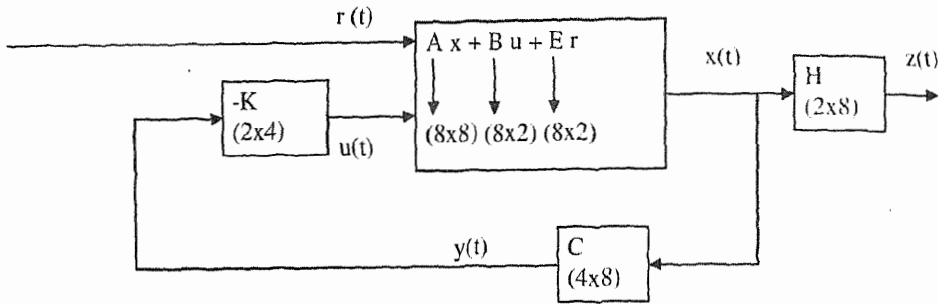
FIG. 4.2. Augmented block diagram for the current control of the PMSM with output feedback.

The performance outputs of the system are $z = [I_{sda}\ I_{sqa}]^T = H.\ x$

Hence the performance output matrix $H = \begin{bmatrix} 0 & 0 & 1 & 0 & 0 & 0 & 0 & 0 \\ 0 & 0 & 0 & 1 & 0 & 0 & 0 & 0 \end{bmatrix}$

The control law is $u = -K.\ y = \begin{bmatrix} V_{sd} \\ V_{sq} \end{bmatrix} = -\begin{bmatrix} K_{pd} & 0 & K_{id} & 0 \\ 0 & K_{pq} & 0 & K_{iq} \end{bmatrix} * \begin{bmatrix} e_{1d} \\ e_{1q} \\ e_{2d} \\ e_{2q} \end{bmatrix}$ (4.6)

where $K = \begin{bmatrix} K_{pd} & 0 & K_{id} & 0 \\ 0 & K_{pq} & 0 & K_{iq} \end{bmatrix}$. It is evident that the PMSM is formulated in the standard form of the LQT with the output feedback.

In practical servomechanisms the torque dynamics will be much faster than the speed dynamics. Moreover, the number of outputs that can be controlled is limited by the number of inputs. So the controller structure is divided into two as in the case of conventional methods, (1) the fast current controller loop and (2) the slower speed control loop. The current controlled loop is a two input -two output system, where as speed controlled system can be treated as a single input single output system. Hence both controllers are designed separately with respective loop dynamics.

Considering the speed control loop, the plant can be approximated as a first order lag corresponding to the mechanical time constant of the rotor. The block diagram for the speed control loop is shown in Fig. 4.3. A lag of 10 msec. is introduced at the speed feedback to account for the speed sensor lag in practical systems. This lag is represented in the form of $1/(1+T_3s)$ where T_3 is the sensor lag. As this is a first order system it is possible to use standard classical SISO techniques to design the speed controller. But this will not yield optimum gains. Therefore the same method used for optimal current controller design is used to design the speed controller also, by formulating it as a LQT problem with output feedback.

The plant dynamics $G_{p\omega}$ is described by matrices $A_{p\omega}$, $B_{p\omega}$, $C_{p\omega}$ and $D_{p\omega}$ where
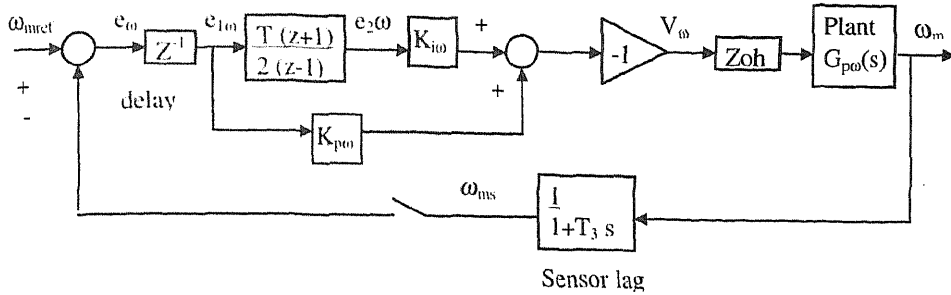
FIG. 4.3. Structure of digital speed controller for PMSM.

$A_{p\omega} = [-B_m/J_m]$; where B_m = friction coefficient; and J_m = rotor mechanical inertia.

$B_{p\omega} = [1/J_m]$; The state of $G_{p\omega}$ is $x_{p\omega} = [\omega_m]$; the input is $u_{p\omega} = [V_\omega]$; and the output is $y_{p\omega} = x_{p\omega}$

The sensor dynamics should be augmented to the plant dynamics. The sensor dynamics G_s can be described by the matrices A_s, B_s, C_s and D_s where

$A_s = [-1/T_3]^T$; $B_s = [1/T_3]^T$; $C_s = [1]$; and $\qquad D_s = [0]$;

The state and output of G_s is $x_s = y_s = [\omega_{ms}]$; and the input is $u_s = [\omega_m]$;

The augmented sensor plant dynamics $G_{\omega s}$ is given by the matrices $A_{\omega s}$, $B_{\omega s}$, $C_{\omega s}$ and $D_{\omega s}$

where $A_{\omega s} = \begin{bmatrix} -B_m/J_m & 0 \\ 1/T_3 & -1/T_3 \end{bmatrix}$; $B_{\omega s} = \begin{bmatrix} -1/J_m & 0 \\ 0 & 0 \end{bmatrix}$; $C_{\omega s} = [0\ 1]$; and $D_{\omega s} = 0$

The states of the augmented plant are $x_s = [\omega_m\ \omega_{ms}]^T$; the input is $u_{\omega s} = u_{p\omega} = [V_\omega]$ the output is $y_{\omega s} = [\omega_{ms}]$;

The continuous domain $G_{\omega s}$ must be transformed into discrete domain and the digital compensator dynamics must be augmented to get the complete system dynamics. It can be noted that the speed control loop is also a full state feedback system. Following the same frame work for current controller design, the speed compensator $G_{c\omega}$ is represented by the matrices $A_{c\omega}$, $B_{c\omega}$, $C_{c\omega}$ and $D_{c\omega}$ where

$$A_{c\omega} = \begin{bmatrix} 0 & 0 \\ T_\omega/2 & 1 \end{bmatrix}; B_{c\omega} = \begin{bmatrix} -1 & 1 \\ -T_\omega/2 & T_\omega/2 \end{bmatrix}; \ T_\omega \text{ is the speed sampling interval.}$$

The states of $G_{c\omega}$ are $x_{c\omega} = [e_{1\omega}\ e_{2\omega}]^T$;

the inputs are $u_{c\omega} = [\omega_{ms}\ \omega_{mref}]^T$; and the outputs are $y_{c\omega} = x_{c\omega}$;

The plant augmented to the compensator and the sensor is denoted by G_ω.

The states of G_ω are $x_\omega = [e_{1\omega}\ e_{2\omega}\ \omega_m\ \omega_{ms}]^T$; the outputs are $y_\omega = [e_{1\omega}\ e_{2\omega}\ \omega_{ms}]^T$; and the inputs are $u_\omega = [\omega_{mref}\ \omega_m\ V_\omega]^T$; The performance output is $z_\omega = H_\omega.x_\omega = [\omega_{ms}]$

Once the system is formulated in the form given in equation (4.5) the optimal speed feed-back gains can be obtained by following the same steps as is done for the optimal current controller design. For variable speed industrial drive applications such as machine tool drive, it is required to have fast response to step change in reference speed without any overshoot. So the speed controller design is aimed at critical damping and the settling time less than 100msec. For fast transient response and limited current, the current controller specifications are decided as $\zeta = 0.707$ and settling time of the current loop should be less than 5 msec.

5. The Optimal controller design

The application of the performance index J to the control system design achieves an optimal system that compromises the minimum state errors and minimum energy criteria. The objective now is to determine the gain matrix K. The optimal feedback gain matrix K can be obtained by minimising the performance index given in equation (3.1) subject to the constraint of the Algebraic Riccati Equation (5.1) for discrete time systems[2] i.e.,

$$A_c^T P A_c - P + Q + C^T K^T RKC = 0 \qquad (5.1)$$

where $A_c = A - B.K.C$ is the closed loop system matrix

P a positive definite symmetric constant matrix.

Now the optimal cost of the system becomes

$$J = \frac{1}{2} tr(P.X) + \frac{1}{2} \sum_i \sum_j \left(g_{ij} . k_{ij}^2 \right) \qquad (5.2)$$

where $X = \bar{x}.\bar{x}^T$ and $\bar{x} = -(A_c - I)^{-1} B_c.r$ is the state at steady state and $B_c = E - B.K F$ is the closed loop input matrix.

The minimisation problem may be solved using one of the numerical techniques available such as SIMPLEX method. With SIMPLEX method we can fix any gain element of the gain matrix K and obtain the optimal gain values for the rest of the elements in the gain matrix by minimising the performance index J. This in fact gives a lot of flexibility in arriving at the stable optimal gains of the PI control structure for the system. Once the system is formulated, the entire optimal control problem can be boiled down to the selection of Q and R matrices to obtain the desired closed loop system response. The steps for obtaining the optimal gain values are as follows.

Step 1: Choice of the initial stabilising gain matrix: As already mentioned in section 5, the optimisation process is an iterative process. Therefore to start with, an initial gain matrix K that makes the closed loop system (A - B.K.C), stable has to be used. The gain can then be optimised by minimising the J. The PMSM and the combination of compensator and PMSM are both open loop stable. If the feedback gains are very small, then the closed loop poles are very close to open loop poles and hence the closed loop system is stable. As a result, the initial proportional gains are set to zero and the integral gains are chosen as 0.01. This will usually provide the system stabilising starting gains for the PMSM, which can be ensured by checking the closed loop eigen values are within unit circle.

Step 2: Choice of state and input weighing matrices Q and R: When the system is formulated as a LQT with output feedback, problem of designing the optimal feedback gain depends on the selection of the Q and R matrices to obtain the desired response of the closed loop system. The translation of specifications into Q and R is imprecise and so selection of Q and R need to be iterative. If the state vector is so selected to have physical significance, then the choice of Q, R entries are more readily reflective of physical insights especially if diagonal Q, R are used. To have control over the closed loop eigenvalues and eigenvectors of a multivariable system, Q is selected as $\rho . H^T.H$. where ρ is a scalar and H is the performance output matrix. If ρ is assigned a large value , the resulting gain leads to a fast response of the system and vice versa. For a multiple input system if R is selected diagonal, the system can tolerate independent gain variations without disturbing stability. But with entries of very different sizes give poor robustness to input cross coupling. So R can be selected as $\mu.d$ where d is a diagonal matrix and μ is scalar. If μ is selected large, the resulting gains K will lead to a slower system response and vice versa.

Step 3: Minimisation of the performance index, J : The performance index $J = 12/.tr(PX)$ is minimised under the constraints of equation (5.1) using the subroutines for SIMPLEX method available in MATLAB. This results in the optimal feedback gain K. The step responses of the system for various values of Q and R are shown in the Figure 5.1. To meet the specification requirements, the gains corresponding to (d) are selected.

The speed responses for step reference corresponding to various Q and R are shown in the Figure 5.2.
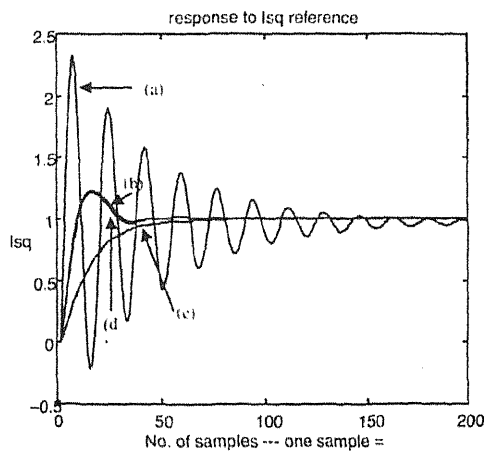
	Kpd	Kid	Kpq	Kiq	Q	R	
(a)	[−6.2837	−473.0893	−23.7608	−169.1319];	0.01*H′.H;	diag [1000	1]
(b)	[−24.3054	−811.7125	−5.6957	−956.25];	0.01*H′.H;	diag [100	1]
(c)	[−29.6732	−687.9348	−2.1968	−285.1706];	0.01*H′.H;	diag [1	1]
(d)	[−24*	−1019.6	−6*	−907.1];	0.01*H′.H;	diag [100	1]

FIG. 5.1. Step response of Isq for different Q and R at $\omega_r = 300$ rad/sec.

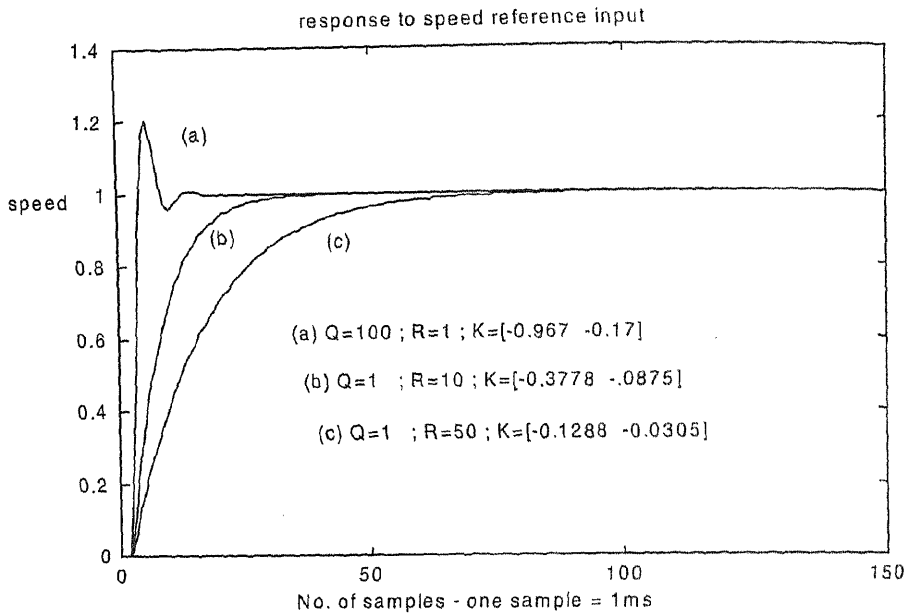response to speed reference input

FIG. 5.2. Step response of rotor speed for various Q and R at 300 rad/sec

6. Torque observer design

Classical controllers employing integral feedback are well known for their by product property of constant disturbance rejection and / or achieving the set point regulation[13]. The idea is that the input to the integrator can asymptotically be zero, yet the output asymptotically constant so as to allow cancellation of the disturbance and / or asymptotic set point reference tracking of the reference 'r'. For set point regulation , there is an external constant reference 'r', and one seek a controller such that the plant output tracks 'r' in the presence of constant unknown disturbances. It is proved that *we can achieve fully the goals of arbitrary set point regulation, only with additional arbitrary constant disturbance inputs*, when the plant matrix is square and with no zero at the origin[12]. In the proposed controller design procedure, the load torque is treated as an external disturbance that can be observed. Hence a disturbance load torque observer is designed to feedforward the extra input required to compensate for the load disturbance at the drive to get robust performance against load torque variations.

For flux vector controlled drives the current control loop time constant is small enough to be neglected (3 ms). Then the machine transient can be represented as

$$J_n.d/dt\ \omega_m + B_n.\omega_m + T_L = K_{Tn}.i_{sq} \tag{6.1}$$

Let $J_n = J_m + \Delta J_m$, $K_{Tn} = K_T = \Delta K_T$, and $B_n = B_m + \Delta B_m$ where J_m, K_T and B_m are nominal values and Δ represents the variations or unknown parameters.

Now the equivalent disturbance torque T_d (s) can be written as[6]

$$T_d(s) = T_L(s) + \Delta B_m.\omega_r(s) + \Delta J_m.s.\omega_r(s) - \Delta K_T.I_{sq}(s) \tag{6.2}$$
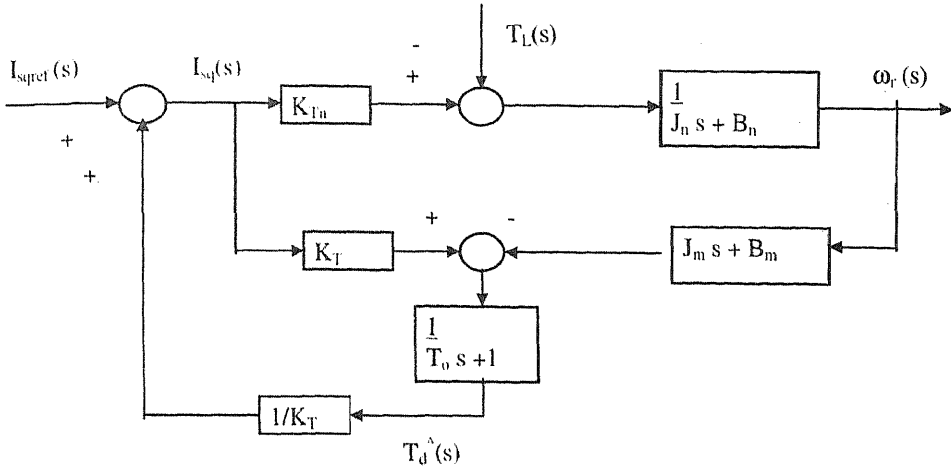
FIG. 6. Block diagram of motor and equivalent disturbance observer

The terms on the right hand side represents the external load torque, torque due to parameter variation and the torque variation due to flux vector control failure and torque ripples respectively. From equations (6.1) and (6.2),

$$T_d(s) = K_T I_{sq}(s) - sJ_m \omega_r(s) - B_m \omega_r(s)$$ (6.3)

The estimate of disturbance torque is constructed by using a low pass filter $[1/(T_o.s+1)]$. This is an observer with T_o as the observer time constant [6]. By block diagram simplification, the following transfer functions are calculated.

$$\frac{\omega_r(s)}{T_L(s)} = -\left(1 - \frac{1}{T_o.s+1}\right)\left(\frac{1}{J_m.s+B_m}\right)$$ (6.4)

Since T_o is very small, $\omega_r(s)/T_L(s)$ becomes zero quickly. Thus the equivalent disturbance has been cancelled by the approximate zeroing method. Now,

$$\frac{\omega_r(s)}{I_{sqref}(s)} = \frac{K_{Tn}}{J_n.s+B_n}$$ (6.5)

shows that the dynamics of the system are not been changed for the controller design point of view.

7. Design of robust controllers for PMSM drive

For designing the optimal controllers, it is assumed that an exact state variable description of the plant to be controlled is available. However in practical situations, the actual and the model plant will never be identical. Some of the parameters such as stator resistance, rotor mechanical inertia, rotor frictional coefficient, may be at variance with respect to that of motor model, which could lead to deterioration in performance and stability. Therefore it is important to consider the stability robustness and performance robustness for designing optimal controllers.

R. MARY LOURDE, *et al.*

The studies on the robustness properties of a stable closed loop system transfer function shows that these properties can be represented in terms of the singular values of sensitivity and complementary sensitivity (cosensitivity) functions[2,12]. The sum of these two functions is an identity matrix. The key results of the study on the relation between these functions and the desired properties are tabulated as shown in Table I. below[12].

where $\overline{\sigma}$ represent the maximum singular value, S is the sensitivity function, $S = (I + G_p G_c)^{-1}$, $T = G_p G_c (I + G_p G_c)^{-1}$; the cosensitivity function and G_p, G_c are transfer functions of plant and compensator respectively. In the present design, it is desired *to keep the tracking error small in the face of the measurement noise*. To ensure small tracking error, $S(j\omega)$ should be small at those frequencies where the reference input $r(t)$ and disturbance $d(t)$ are large. This will yield good disturbance rejection. On the other hand, for satisfactory sensor noise rejection, the cosensitivity $T(j\omega)$ should be small at high frequencies say at ω_n[2,12].

This is guaranteed if $\overline{\sigma}(G_{pa}G_c) << 1, for \omega > = \omega_n$ (7.1)

To guarantee stability robustness in the face of plant modelling uncertainty, it is given that the cosensitivity $T(j\omega)$ should be bounded above by the reciprocal of the multilplicative modelling discrepancy bound $m(\omega)$. i.e.,

$$\overline{\sigma}(T(j\omega)) < 1/ m(\omega) \qquad (7.2)$$

If the worst case uncertainties in the parameters like stator resistance, rotor mechanical inertia, rotor frictional coefficients etc. are known, then the upper bound $m(\omega)$ can be found from

$$M(j\omega) = (G_p^* - G_p) G_p^{-1} \qquad (7.3)$$

$$m(j\omega) = \overline{\sigma}(M(j\omega)) \qquad (7.4)$$

where G_p^* represents the actual plant.

In this paper, the worst case uncertainties in the parameters considered are 50% to 500% of rotor inertia, 50% to 150% of stator resistance and friction coefficients. Normally the stator resistance variations of a PMSM are very small, less than 10% of the nominal value and the stator leakage inductance variation is almost nil.

The Fig.7.1 shows the stability robustness graph of the inner current loop of the PMSM servo drive considering the assumed worst case uncertainties in the parameters at a rotor speed of 300 rad/sec. Fig. 7.2 (a) and (b) shows the stability robustness of the outer speed loop of the

Table I

The role of sensitivity and complementary sensitivity in classical control

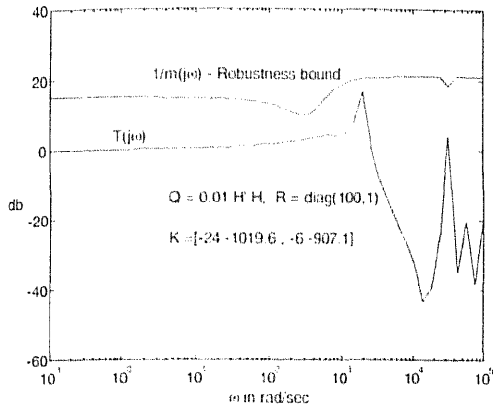| Property desired	S or T constraints
Tracking	$\overline{\sigma}$ (S) small
Disturbance suppression	$\overline{\sigma}$ (S) small
Noise suppression	$\overline{\sigma}$ (T) small
Control magnitude limitation	$\overline{\sigma}$ (S) not small when $\overline{\sigma}$ (G_p) is small $\overline{\sigma}$ (S) small
Sensitivity to *structured plant parameter variations*	$\overline{\sigma}$ (S) small
Sensitivity to *unstructured multiplicative uncertainty*	$\overline{\sigma}$ (T) small

FIG.7.1. Stability robustness bound and max. singular value of cosensitivity T(jω) of current loop with Rs 150% and Ls 110% at w$_s$ = 300 rad/sec.
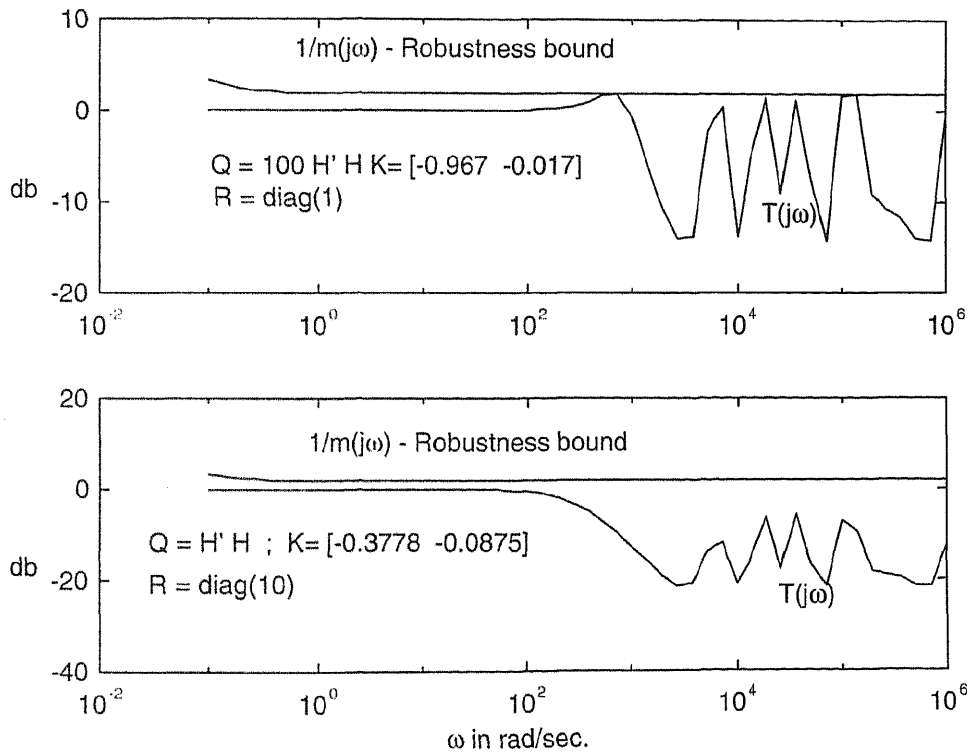

FIG. 7.2. Stability robustness of speed loop with 500% J$_m$ and 150 % B$_m$ at ω = 300 rad/sec.

PMSM drive using different values of optimal gains at 300 rad/sec. As seen from the equation (4.1), since ω$_s$ also forms a part of the system matrix, the matrix A as well as the optimum feed-
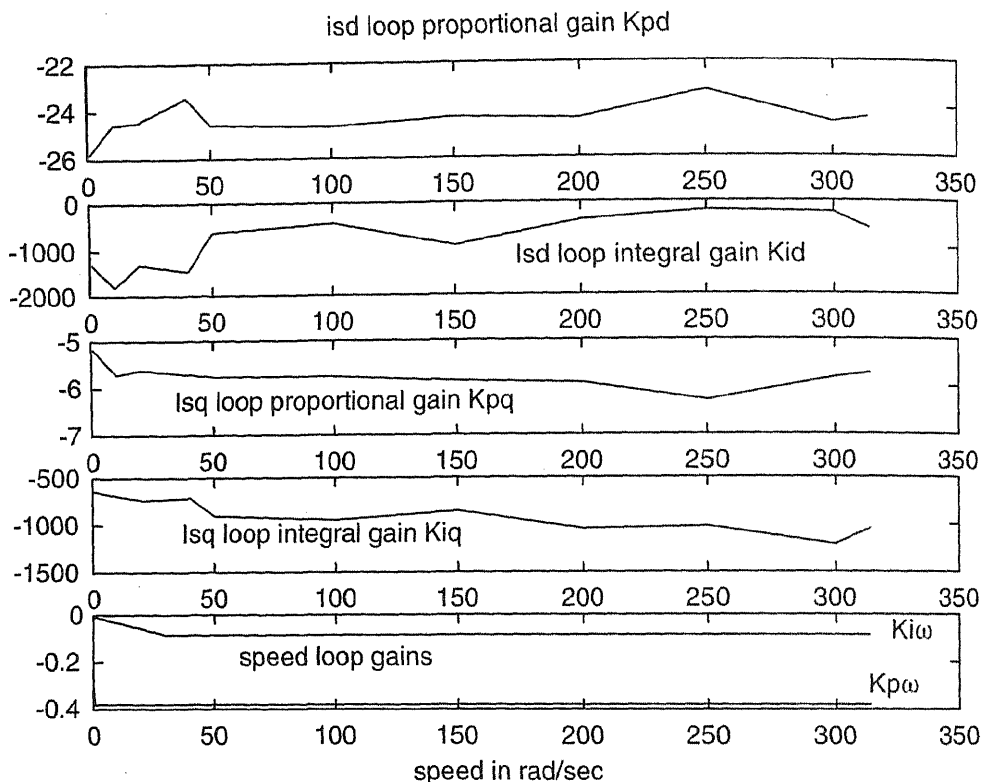
isd loop proportional gain Kpd

FIG. 7.3 Optimal controller gains at various speeds

back gains of the system will vary with ω_s. Hence the robust optimal feedback gains of the PI controllers should be found at various speeds. Accordingly, the optimal controller gains computed at various rotor speeds are pictorially represented in the Fig. 7.3.

The gains corresponding to speeds other than that marked in the Fig. 7.3 can be obtained through interpolation.. Alternately, a constant feedback gain which is optimum for a particular speed (for example corresponding to the rated speed) can also be used for other reference speeds. But these gains may not be optimum at other reference speeds. However they result in stable closed loop system for PMSM drive over the entire range of speeds. It is verified and an example is shown in Fig. 7.4. The Fig. 7.4 illustrates the stability robustness of the inner current loop of the PMSM drive at different speeds using the optimal controller gains corresponding to a reference speed of 300 rad/sec. It is evident from the Fig. 7.4 that even though the magnitude of the robustness bound change with rotor speeds, the maximum singular value of the cosensitivity function $T(j\omega)$ is well with in the bound and hence the closed loop system is stable at all speeds.

The Fig. 7.5 shows the stability robustness of the speed loop in the face of the motor mechanical parameter variations at different speeds using the gains corresponding to the rotor
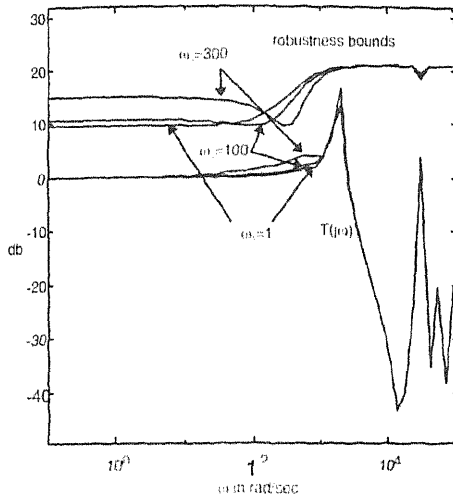
FIG. 7.4. Stability robustness of the drive with R, 150% and L, 110% at various speeds using the optimal gains corresponding to ω = 300 rad/sec.
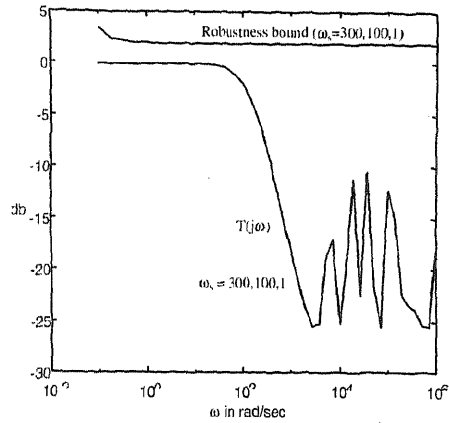
FIG. 7.5. Stability robustness of the drive with J_m 500% and B_m 150% at various speeds using the optimal gains corresponding to ω, = 300 rad/sec.

speed of 300 rad/sec. It is found that for the speed loop, the effect of using constant speed feedback gains at all speeds on the stability robustness is almost nil.

From Fig. 7.4 it is noted that using the gains corresponding to higher speeds than the reference speeds, increases the stability robustness of the drive. However, stability robustness of the drive is decreased when using the gains corresponding to lower speeds than the reference speed. Hence if one need to use a constant feedback gain for the entire range of reference speeds, the gains corresponding to the rated or maximum speed can be used while ensuring the stability of the closed loop system.

8. Simulation results

The simulation results using the optimal PI controller is shown in Figure 8.1. The motor is given a reference speed of 300 rad/sec. and it is disturbed with a load torque of 5 Nm. at 0.4 sec. and the load is released at 0.7seconds. The results are shown in Figure 8.1.

The effect of motor parameter variations with optimal controller is simulated and is shown in Figure 8.2(a) and (b) below.

It shows that the controller has good disturbance rejection and is robust against parameter variations. The variations in mechanical constants such as moment of inertia and friction coefficient affects the speed of transient response. From the simulation results it can be noted that for the variations in moment of inertia and friction coefficient that are the most likely parameters at variance, the optimal controller gives very small variation in output therefore it is robust. The performance of the controllers at low speeds are illustrated in Figures 8.3.
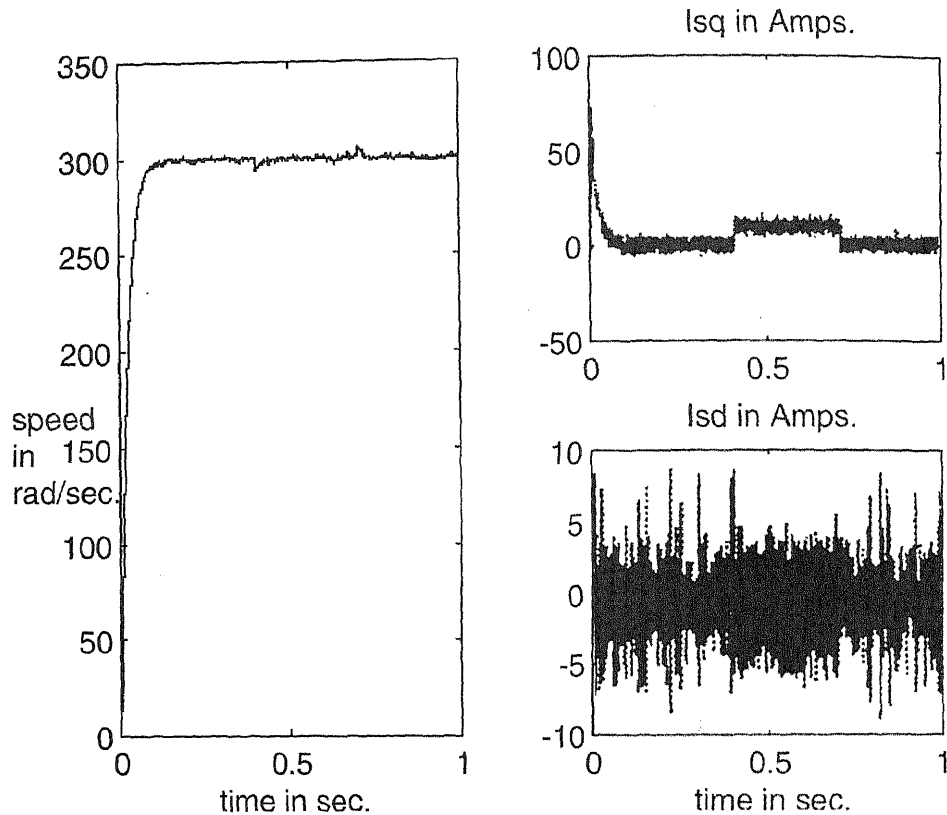
FIG. 8.1. Response of the drive using optimal controllers

9. Conclusions

The structure of the controller being fixed as Proportional-Integral (PI), the algorithm for tuning the controller parameters based on optimal control theory is illustrated. The performance of the controllers applied to a PMSM servo drive were studied. The results show that the change in speed due to a load torque disturbance and the steady state error is absolute irrespective of the motor running speeds. The simulation results also show that with the PI controller designed using optimal control methods, desired time domain specifications can be achieved for step changes in the reference speed.

Frequency domain information is very useful in output feedback design methods for determining robustness to disturbances and stability in the face of unmodelled dynamics. It also assists in deciding the fineness of the gain scheduling such as low frequency bounds for the parameter variations as the state varies from the nominal operating point. While the classical control method concentrates primarily on the tracking problem, the optimal control method concentrates both on the tracking and regulation problem. Also in optimal control methods, constraints
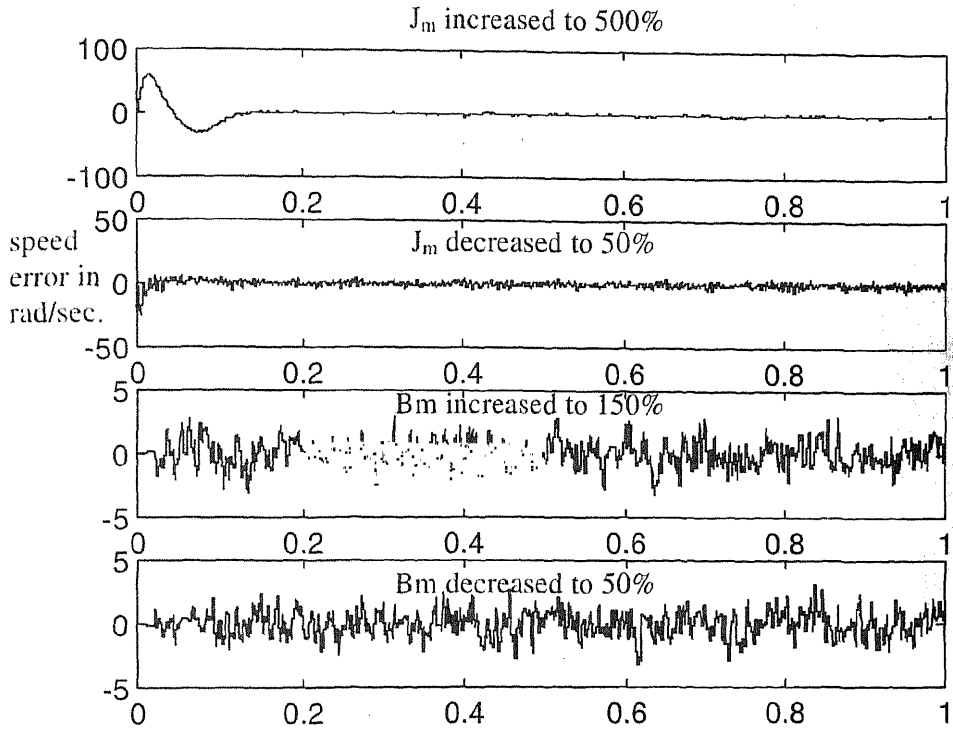
J$_m$ increased to 500%

J$_m$ decreased to 50%

speed error in rad/sec.

Bm increased to 150%

Bm decreased to 50%

FIG. 8.2(a) Effect of change in J$_m$ and B$_m$ with optimal controllers

Ls increased to 110%

Ls decreased to 90%

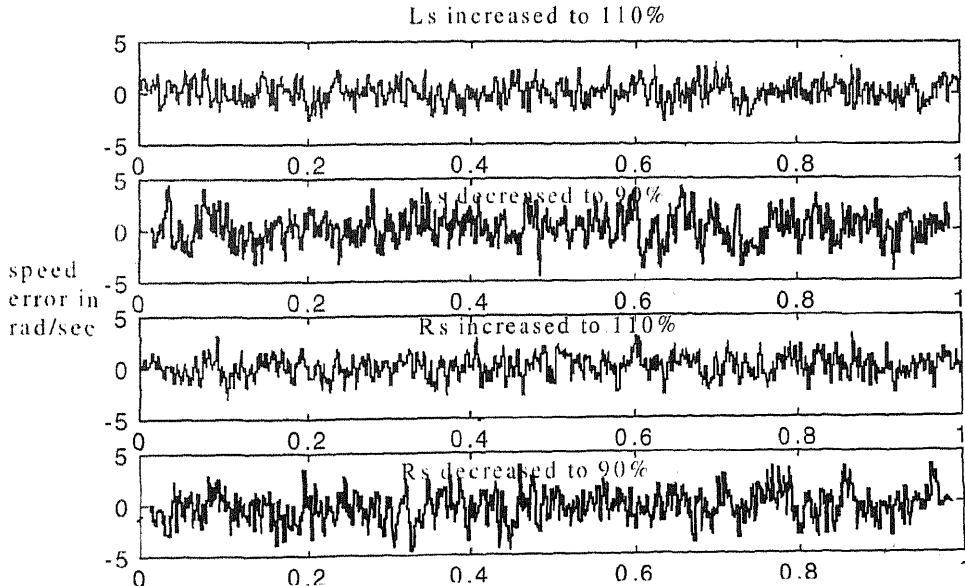speed error in rad/sec

Rs increased to 110%

Rs decreased to 90%

FIG. 8.2(b). Effect of variations in L$_s$ and R$_s$
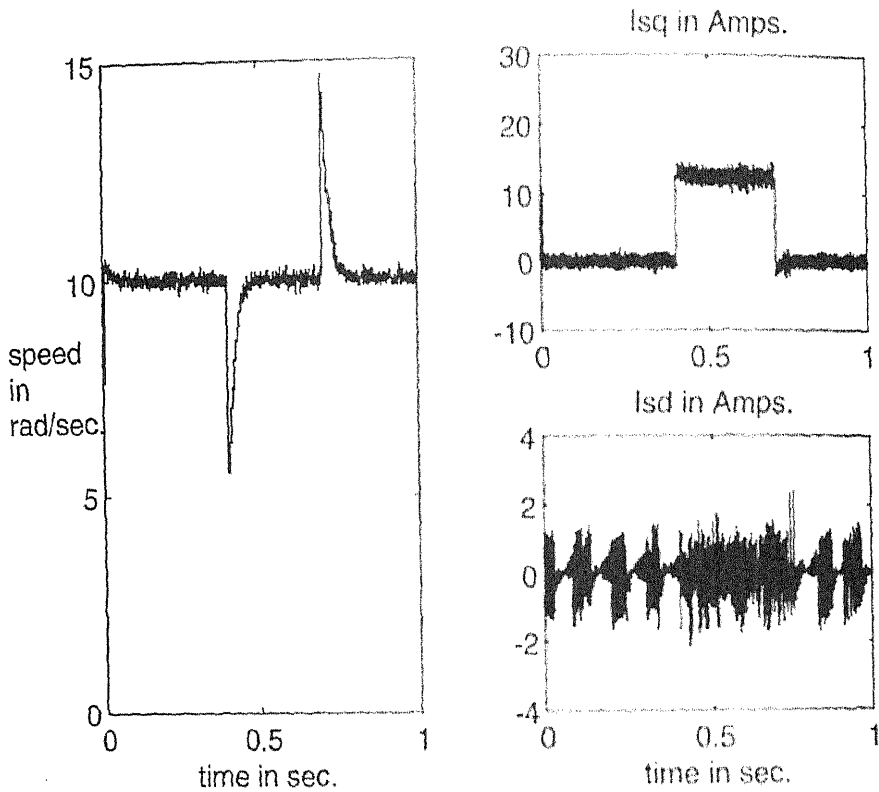
FIG. 8.3. Performance of the servo drive with optimal speed controller at ω = 10 rad/sec

specified on the problem can be directly considered, whereas in the classical design methods, there is no systematic way of handling constraints.

Appendix I : Motor parameters used

R_s = 0.98 ohm/phase; L_s = 8.035 mH/phase; J_m = 21 e-04 Nm/rad/s;

B_m = 5e-4 Nm/rad/s; K_E = 0.612 v/rad/sec; K_T = 0.4093 Nm/A;

Nominal speed = 3000 rpm; Nom. current = 10.4 A; Nom. torque = 9 Nm.

Appendix II : List of symbols used

R_s, L_s — stator resistance and leakage inductance

V_{sd}, I_{sd} — direct axis voltage and current

V_{sq}, I_{sq} — quadrature axis voltage and current

K_E — back-emf constant (volts/rad)

K_T — torque constant (Nm/A)

ω_r, ω_s --rotor speed ,synchronous speed in radians/sec

T_d, T_L --developed and load torque

J_m, B_m --moment of inertia and damping coefficient of the motor

References

1. LEONHARD, W.,   Control of Electrical Drives, Springer Verlag, 1985.

2. FRANK L. LEWIS,   Applied optimal control and estimation, Prentice Hall, 1992.

3. PILLAY, P. AND KRISHNAN, R.,   Modelling, Simulation, and Analysis of Permanent Magnet Motor Drives, Part I: The permanent magnet synchronous motor drive, *IEEE Trans. on IA*, vol.25, **2**, 1989, pp. 265–273.

4. UMANAND, L.,   Modelling and simulation studies on parameter adaptation and digital controller synthesis for vector controlled AC drives, Ph.D. dissertation , CEDT, IISc., India.1994.

5. LOW, T. S., LEE, T. H. AND CHANG, K. T.   An optimal speed controller for permanent-magnet synchronous motor drives, *IEEE Trans. on IE*, vol. 41, **5**, 1994, pp. 503–510.

6. SUNTINO, A., FURKAWA, J., KOBAYASHI, H. AND DOTE, Y.,   Variable structured robust controller by fuzzy logic for servo motors, *IEEE Trans. on IE*, Vol. 40, 1, 1993, pp. 80–87.

7. DAVISON, E. J., AND FERGUSON, I. J.,   The design of controllers for the multivariable robust servomechanism problem using parameter optimisation methods, *IEEE Trans. on Automatic Control*, vol.AC-26, **1**, 1981, pp. 93–110.

8. RAJARAM, S., PANDA, S. K., AND SANG, L. K.   Performance comparison of feedback linearised controller with PI controller for PMSM speed regulation, *IEEE PEDES '96*, pp. 353–358.

9. GRCAR, B., CAFUTA, P., ZNIDARIC, M., AND GAUSCH, F.,   Non-linear control of synchronous servo drive, IEEE Tans. on Control system technology, vol.4, **2**, 1996, pp 177–184.

10. SHAKED, U.,   Guaranteed stability margins for the discrete-time linear quadratic optimal regulator, *IEEE Trans. on Automatic control vol.AC-31*, 2, 1986, pp. 162–165.

11. HO, W. K., GAN, O. P., TAY, E. B., AND ANG, E. L.,   Performance and Gain and Phase margins of well-known PID tuning formulas, *IEEE Trans. on Control system technology*, vol.4, **4**, 1996, pp. 473–477.

12. ANDERSON, B. D. O., JOHN B. MOORE,   Optimal control, Linear Quadratic methods, PHI,1991.